# Dark Matter or Neutrino recoil? Interpretation of Recent Experimental Results.

Maxim Pospelov[1,2] and Josef Pradler[3]

[1]*Perimeter Institute, Waterloo, Ontario N2L 2Y5, Canada*
[2]*Department of Physics and Astronomy, University of Victoria, Victoria, BC, V8P 5C2, Canada*
[3]*Department of Physics and Astronomy, Johns Hopkins University, Baltimore, MD 21210, USA*

The elastic nuclear recoil signal, being under intense scrutiny by multiple underground experiments, can be interpreted either as coming from the interaction of nuclei with WIMP dark matter or from the scattering of new species of MeV-energy neutrinos. The most promising model for the latter case is a neutrino $\nu_b$ that interacts with baryon number, and with a flux sourced by the oscillations of regular solar $^8$B neutrinos. We re-analyze this model in light of the latest experimental results. In contrast to the light-DM interpretation of various tentative positive signals (anomalies) that is now seriously challenged by the negative results of the LUX experiment, the neutrino interpretation remains a viable explanation to most of the anomalies. Considering future prospects, we show that the superCDMS experiment alone, when equipped with Ge *and* Si detectors, will be able to detect $\nu_b$ and discriminate the model from a light DM interpretation. In addition, we also provide the forecast for the new CRESST-II run that now operates with new detectors and diminished backgrounds.

arXiv:1311.5764v1 [hep-ph] 22 Nov 2013

## INTRODUCTION

The search for a non-gravitational detection of dark matter (DM) has entered a new phase with more and more experiments reporting their results at ever increasing limits of sensitivity. Indeed, if DM is composed of weakly interacting massive particles (WIMPs), there is a real chance that occasional events of WIMP-atom scattering may be recorded in low-background experiments [1]. The weakness of DM-nucleus scattering can only be compared to neutrino detection, which is also very challenging on the account of a neutrino's weak interaction with ordinary matter. Necessarily then, sensitive neutrino and WIMP detectors usually consist of fairly large target mass, and due to the simplicity of the underlying event (*e.g.* nuclear recoil) register only few channels. This stands in sharp contrast with particle physics experiments at colliders, where, given enough complexity and sophistication of detectors, hundreds and thousands of channels can be registered as part of one event. Given the rather simple form of WIMP scattering events, even in the case of a positive signal detection, there will be a serious challenge in distinguishing it from other potential origins of nuclear recoil. One idea that has been put forward recently [2–4] shows that the current generation of WIMP detectors is also sensitive to the combination of non-standard neutrino oscillation and interactions, especially in the regime of recoil similar to that created by relatively light, 10 GeV and less, WIMP particles. Moreover, it has been suggested that some [2, 4] (if not all) of the existing hints on a positive signal can be explained within the model of an extra neutrino species that interacts with the baryonic current.

The purpose of this paper is to revisit this idea, and to give an update to the interpertation of a variety of direct DM detection experimental results in terms of the recoil of a new neutrino species that originates from ordinary solar neutrinos due to oscillation. Since our last publication on the subject [4], there has been a series of developments in the field, notably a new excess of events reported by the CDMS-II collaboration for their silicon-made detectors [5], and a negative result from the LUX experiment [6] that strongly disfavors the interpretation of many anomalies as a WIMP DM signal [7, 8]. Given the immense amount of both experimental and theoretical interest to the subject, and especially to the light WIMP interpretations of the direct detection anomalies, it is important to understand the status of alternative explanations for the signal.

This paper is organized as follows: In the next two sections we give an overview of the neutrino oscillation portal idea, and introduce the model for a new neutrino neutrino $\nu_b$ that has stronger-than-weak interaction strength $G_B$ with the baryonic current. After that we adress new experimental results, one by one, discussing implications of the liquid xenon experiments [6, 9, 10], CDMS-II silicon [5], and CoGeNT [11, 12]. The next-to-last section discusses details of how the recoil of $\nu_b$ states and light dark matter can be distniguished in practice, given more statistic planned for the new run of CRESST-II[13], and making projections for superCDMS [14].

## NEUTRINO OSCILLATION PORTAL

Considering a light fourth neutrino, we have two limiting cases what regards the mass splitting relative to the three, mostly active flavors.

1. Sizable mass squared differences $|\Delta m^2_{4i}| \gg |\Delta m^2_{ij}|$ for $i,j = 1,2,3$. This scenario is typically considered in the context of the short baseline anomalies LSND [15], MiniBooNE [16], and the deficit of reactor neutrinos; see [17] and references therein. In the presence of enhanced interactions, this scenario is difficult to reconcile with observations: matter effects will likely have a substantial impact on the

flavor evolution, and enhanced values of a new interaction will be tightly constrained by the total counting rate of neutrino-related events.

2. A new state that is (nearly) degenerate with one of the SM massive neutrinos $n_i$, $\Delta m^2 \equiv |\Delta m^2_{4i}| \ll |\Delta m^2_{ji}|$ for $j \neq i, 4$. In this case the classification into short- and long-baseline neutrino experiments will remain largely intact; $\Delta m^2$ becomes the controlling parameter of flux in the new flavor $\nu_b$ generated from oscillation. We will show that in the limit of $\Delta m^2 \to 0$ the flux in the fourth state that would be generated from oscillation can vanish altogether. Therefore, there is always a choice of $\Delta m^2$ small enough that there is no impact on any of the neutrino oscillation experiments other than via pair-production of $\nu_b$.

We shall pursue option (2) in the following and call it the "neutrino oscillation portal."

We start from the general expression of flavor conversion probabilities $P_{\beta\alpha}(t) \equiv |\langle\nu_\beta|\nu_\alpha(t)\rangle|^2$ for $N$ neutrinos $|\nu_\alpha\rangle$ that related to their mass eigenstates $|n_i\rangle$ via the unitary transformation $|\nu_\alpha\rangle = \sum_{i=1}^N U^*_{\alpha i}|n_i\rangle$. Let us consider a hierarchy of masses between two groups $A = \{n_1, \ldots, n_{N_A}\}$ and $B = \{n_{N_A+1}, \ldots, n_N\}$ and assume baselines such that phases among respective group members are negligible. Then, there is only one common dominating phase, namely, between members of $A$ and $B$, $\phi_{AB} \simeq \Delta m^2_{AB} L/(2E_\nu)$; $L \simeq ct$ is the propagation distance and $E_\nu$ is the relativistic neutrino energy. The appearance probability is then given by,

$$P_{\beta\alpha} = \left|\sum_k U^*_{\alpha k} U_{\beta k} \exp\left(-i\frac{\Delta m^2_{k1} L}{2E_\nu}\right)\right|^2 = \sin^2\left(2\theta^{\rm eff}_{\beta\alpha}\right)\sin^2\left(\frac{\Delta m^2_{AB} L}{4E_\nu}\right) \quad (\alpha \neq \beta), \qquad (1)$$

where the second relation is written in analogy to the two-flavor case. The sine-squared of the effective angle reads (see, *e.g.* [18]),

$$\sin^2\left(2\theta^{\rm eff}_{\beta\alpha}\right) = 4\left|\sum_{k>N_A} U^*_{\alpha k} U_{\beta k}\right|^2. \qquad (2)$$

One can replace $\sum_{k>N_A}$ with $\sum_{k<N_A+1}$ because of unitarity of $U$.

Oscillation from $\alpha = e, \mu, \tau$ into a *new* state $\beta = b$ is protected if the transition amplitude vanishes to desired accuracy, $\sin^2(2\theta^{\rm eff}_{b\alpha}) = 0$. This can be achieved as follows: Consider, for concreteness, the case of four light neutrinos $n_{1,\ldots 4}$ and adopt the notation in which $n_{1,2,3}$ are mostly SM states, with PMNS-like mixing matrix $V_3$, and in which $n_4$ is mostly $\nu_b$. Then, the unitary $4 \times 4$ mixing matrix $U$ can be defined as a product, such, that $V_3$ stands to the left of new rotations $R_{i4}$ in the $i4$ plane by angles $\theta_{i4}$,

$$U = V_3 \prod_{i=1}^3 R_{i4}(\theta_{i4}). \qquad (3)$$

If all new angles $\theta_{i4}$ between the groups $A$ and $B$ for which a non-negligible phase $\phi_{AB}$ exists are zero, then, indeed, $\sin^2(2\theta^{\rm eff}_{b\alpha}) = 0$. This gives rise to the notion of what we shall call the "neutrino oscillation portal."

In the following, we shall consider the case $A = \{n_1, n_2, n_4\}$ and $B = \{n_3\}$ and assume a fine mass splitting $\Delta m^2 < 10^{-8}\,{\rm eV}^2$ between $n_2$ and $n_4$. Keeping only one mixing angle $\theta_b = \theta_{24} \neq 0$, $\theta_{14}, \theta_{34} = 0$ the fourth neutrino $n^0_4$ is mixed into $n^0_2$ as a small perturbation, such that $n_{2,4}$ are the true propagating fields,[1]

$$n_2 = \cos\theta_b n^0_2 - \sin\theta_b n^0_4, \quad n_4 = \sin\theta_b n^0_2 + \cos\theta_b n^0_4.$$

In this scenario, one finds of the vacuum transition probabilities from flavor $\alpha = e, \mu, \tau$ into $\nu_b$

$$P_{b\alpha} < 10^{-4} \quad \text{for} \quad L \leq 10^3\,{\rm km}, \qquad (4)$$

which holds for $E \geq 1\,{\rm MeV}$ and any value of $\theta_b$.[2] Hence, the new interaction $G_B$ (see below) is protected for $G_B/G_F \lesssim 10^4$ from laboratory probes on any terrestrial baselines; matter effects will not spoil the decoupling of the fourth neutrino state in the $\Delta m \to 0$ limit.

To illustrate the convenience of the parameterization (3) consider the opposite definition, $\tilde{U} = R(\tilde{\theta}_{24})V_3$ together with the appearance probability of $\nu_b$ from a muon neutrino beam when atmospheric splitting dominates,

$$\sin^2 2\tilde{\theta}^{\rm eff}_{b\mu} = \cos^4\theta_{13}\sin^4\theta_{23}\sin^2 2\tilde{\theta}_{24} \quad (\tilde{\theta}_{14}, \tilde{\theta}_{34} = 0).$$

Here, $\nu_b$ appearance is not protected by a mass-splitting unless a special combination with additional new angles $\tilde{\theta}_{14}, \tilde{\theta}_{34} \neq 0$ is chosen, obscuring the decoupling in the $\Delta m \to 0$ limit.

While the idea explored in this paper uses mass splittings that are comparable to the earth-sun distance, one could also entertain a more radical use of the "neutrino oscillation portal", when *e.g.* neutrinos of astrophysical origin oscillate into the more interacting counterparts [20], leading to interesting phenomenological consequences that wait to be explored. Also, our framework

---

[1] The relation between fields is $\vec{\nu} = U\vec{n}$ and we have used the notation $\vec{n}^0 = V_3^\dagger \vec{\nu}$ where we imagine $V_3$ quadratic and diagonal in the fourth state.

[2] We have used SM angles $\sin^2(2\theta_{12}) = 0.86$, $\sin^2(2\theta_{23}) \simeq 1$, $\sin^2(2\theta_{13}) = 0.09$ in the standard parameterization of $V_3$ and $|\Delta m^2_{31}| \simeq 2.3(1) \times 10^{-3}\,{\rm eV}^2$ and $\Delta m^2_\odot = \Delta m^2_{21} \simeq 7.5(2) \times 10^{-5}\,{\rm eV}^2$ for atmospheric and solar mass squared splittings, respectively; see [19]. Once $\theta_{24}$ becomes $O(1)$ a three-flavor analysis from which these parameters are inferred from is not strictly self-consistent.

is, of course, broader than the 4-neutrino states. One could also contemplate modifications to this model by the presence of several new neutrino states, where only part of them have enhanced interactions. This way one may also accommodate an explanation of the short base line anomalies.

## BARYONIC NEUTRINOS

Here we consider gauged baryon number and a new left-handed neutrino which is charged under $\mathrm{U}(1)_B$. The covariant derivatives of the baryonic neutrino $\nu_b$ and of the quark fields $q$ are,

$$D_\mu \nu_b = (\partial_\mu + i q_\nu g_B V_\mu)\nu_b, \tag{5}$$

$$D_\mu q = \left(D_\mu^{\rm SM} + i q_B g_B V_\mu\right) q. \tag{6}$$

$g_B > 0$ is the $\mathrm{U}(1)_B$ gauge coupling and $q_\nu = \pm 1$ and $q_B = 1/3$ are the charges of $\nu_b = \frac{1}{2}(\mathbb{1} - \gamma^5)\nu_b$ and quarks $q$, respectively; $|q_\nu| \neq 1$ can be reabsorbed into the value of $g_B$. For $q_\nu = 1$ and $\theta_b < \pi/4$, the MSW condition can only be met by $\bar{\nu}_b$ [2–4]. $V_\mu$ mediates the interaction, which carries mass $m_V$ from the Higgsing of $\mathrm{U}(1)_B$ or from a Stueckelberg mechanism. Notice that the gauge anomaly in the model can be cancelled due to new fermionic states at the electroweak scale.

It is useful to measure the new interaction in units of Fermi's constant. We define,

$$G_B \equiv \frac{q_\nu g_B^2}{m_V^2} \approx 10^5 G_F \times q_\nu g_B^2 \left(\frac{1\,\mathrm{GeV}}{m_V}\right)^2. \tag{7}$$

Invariably, a sizable enhancement, $G_B/G_F \gg 1$, requires $m_V$ to be well below the weak scale. As it turns out, the "safest" phenomenological choice is $m_V$ in the $\sim O(1-100)$ MeV range, where $g_B$ can be quite small, below 0.01, and indeed difficult to detect despite kinematic accessibility for many experiments; see, *e.g.* [21].

In the previous works [2, 4] an effective enhancement factor was defined,

$$\mathcal{N}_{\rm eff}^2 \equiv \frac{1}{2}\left(\frac{G_B}{G_F}\right)^2 \sin^2 2\theta_b \simeq 2\theta_b^2 \left(\frac{G_B}{G_F}\right)^2, \tag{8}$$

such that for low-energy processes, in the limit of rapid oscillations, one can make the identification $P_{b\alpha} G_B^2 \to \mathcal{N}_{\rm eff}^2 G_F^2$. Together with the mass splitting, the effective enhancement factor defines a simple two-parameter space $\{\Delta m,\, \mathcal{N}_{\rm eff}\}$ that we are set to explore in connection with the direct detection experiments.

While the baryonic portal is not unique, as one could also consider interactions with electric charge via the more familiar "photon kinetic mixing" portal, phenomenologically such option seems to be less attractive. Indeed, new neutrino states appearing through the oscillation of solar neutrinos are also constrained by their neutral-current type inelastic interactions with nuclei. As shown in [2], the baryonic current portal is by far the least constrained choice, while the kinetic mixing portal may not be allowed at an interesting level of $\mathcal{N}_{\rm eff}$. Finally, $\nu_b$ is also a safe option when it comes to cosmological aspects [2, 22].

## DIRECT DETECTION

The spin-independent elastic recoil cross section on nuclei can be obtained from the usual active neutrino-nucleus coherent scattering [23] using the replacement $G_F^2 (N/2)^2 \to G_B^2 A^2$ [2]. In terms of a recoil cross section,

$$\frac{d\sigma_{\rm el}}{dE_R} = \frac{G_B^2}{2\pi}\, A^2 m_N F^2(|\mathbf{q}|) \left[1 - \frac{(E_{\rm min})^2}{E_\nu^2}\right], \tag{9}$$

where $E_{\rm min} = \sqrt{E_R m_N/2}$ is the minimum energy required to produce a recoiling nucleus of mass $m_N$ and kinetic energy $E_R$. $A$ is the atomic number of the nucleus, and the nuclear form factor suppression is given by $F^2(|\mathbf{q}|)$ for scatterings with momentum transfer $\mathbf{q}$. We employ the Helm parametrization [24] with the nuclear skin thickness of 0.9 fm.

As it turns out, $^8$B neutrinos from the sun have the best combination of large flux and high end-point energy, $\Phi_{^8\mathrm{B}} = (5.69^{+0.173}_{-0.147}) \times 10^6\,\mathrm{cm}^{-2}\,\mathrm{s}^{-1}$, and $E_{\rm max} = 16.36\,\mathrm{MeV}$ [25], respectively. The MSW solution to the solar neutrino problem operates on the highly energetic part of the neutrino spectrum so that $\nu_e$ exit the sun mostly as $n_2$. It is precisely this part of the spectrum that is relevant for producing nuclear recoils above detection thresholds. With $\theta_b = \theta_{24} \neq 0$ the appearance probability from the solar $\nu_e$ flux in the tri-bimaximal mixing approximation is given by [2],

$$P_{be}(L, E_\nu) \simeq \sin^2(2\theta_b)\sin^2\left[\frac{\Delta m^2 L(t)}{4E_\nu}\right]. \tag{10}$$

The theoretical recoil spectrum arising form a solar $\nu_b$ flux is given by a convolution of the recoil cross section (9) with the neutrino differential flux $df/dE_\nu$ weighted by $P_{be}$,

$$\frac{dR}{dE_R} = N_T \left[\frac{L_0}{L(t)}\right]^2 \Phi_{^8\mathrm{B}} \int_{\mathrm{E_{min}}}^{\mathrm{E_{max}}} dE_\nu\, P_{be}(t, E_\nu) \frac{df_i}{dE_\nu}\frac{d\sigma_{\rm el}}{dE_R}. \tag{11}$$

We have included an overall flux modulation factor $[L_0/L(t)]^2$ due to the earth's eccentric orbit (ellipticity $\epsilon = 0.0167$) around the sun with a maximum at perihelion on ∼Jan 2 and $L_0 = 1$ AU. For $df/dE$ we take the $^8$B flux from [26, 27]; $\int dE\, df_i/dE = 1$. $N_T$ denotes the number of target nuclei per unit detector mass.

Equipped with the necessary theoretical quantities we now turn to those experiments which have either released

new data or received significant upgrades in their understanding of detector and signal; for details on other searches and how their results are translated to the $\nu_b$ model we refer the reader to our previous work [4].

### Xenon experiments

Rare underground event searches based on liquid/gaseous xenon two-phase experiments have advanced to the workhorses of DM direct detection. The advantage lies in scale-ability and the fiducialization of detector mass.

Discrimination between nuclear and electron recoils is achieved by measuring prompt (S1) and delayed (S2) scintillation light. The latter is due to drifting ionized electrons into the gaseous phase. Nuclear recoil energies are obtained from

$$\mathrm{S1} = E_R \mathcal{L}_{\rm eff}(E_R) L_y \frac{S_n}{S_e}, \qquad \mathrm{S2} = E_R Q_y(E_R) Y, \quad (12)$$

measured in units of photo-electrons (PEs). Only a small fraction of the deposited recoil energy is emitted in form of prompt scintillation light S1. It determines the discrimination threshold and relies upon the scintillation efficiency $\mathcal{L}_{\rm eff}$ for nuclear recoils relative to electron recoils; $L_y$ is the light yield in PEs/keVee of a $\gamma$-calibration source and $S_e$ and $S_n$ are experiment-specific quenching factors for scintillation light due to electron and nuclear recoils, respectively. $Q_y$ is the ionization yield per keV nuclear recoil and $Y$ is the measured number of PEs produced per ionized electron which is an amplification factor.

#### *LUX*

The Large Underground Xenon (LUX) experiment located at the Sanford Underground Research Facility has very recently published its first DM data from 85.3 live days with a fiducial target mass of 118 kg [6]. A total of 160 events were observed in the S1 acceptance region $2-30$ PE, consistent with electron-recoil (ER) background from radioactive contamination. LUX is now the leading experiment in the search for DM spin-independent scatterings, excluding a cross section of $8\times10^{-46}\,\mathrm{cm}^2$ at DM mass 33 GeV.

Limits on the $\nu_b$ signal are derived as follows. We first compute the expected S1 signal from $\nu_b$ using the absolute light yield estimation (the quantity $\mathcal{L}_{\rm eff} L_y S_n/S_e$) of [28, 29]. Conservatively, a hard cut is introduced at $E_R = 3\,\mathrm{keV}$. Next we account for the Poisson nature of the process and retain events in the S1 acceptance window $2-30$ PE. The signal is then binned in accordance with supplementary Fig. 8 which reports observed and ER-background rates as a function of S1. This allows us to account for expected background $\nu_{\rm bg}$ and we use the first five bins $N_{\rm bins}=5$ with $S1 \lesssim 26$ PE where $\nu_b$-signal $\nu_{\rm s}$ is present; $\nu = \nu_{\rm s} + \nu_{\rm bg}$. A value of $\mathcal{N}_{\rm eff}$ is excluded in each bin at a level $1-\alpha_{\rm bin}$ if the probability to see as few as $n_{\rm obs}$ Poisson-distributed observed events is $\alpha_{\rm bin} = \sum_{n=0}^{n_{\rm obs}} \nu^n \exp(-\nu)/n!$. The overall exclusion limit is obtained by including a statistical penalty for observing more than one bin, $1-\alpha = (1-\alpha_{\rm bin})^{N_{\rm bin}}$.

The resulting constraint is shown in Fig. 3 by the thick solid line. Its modulation in $\mathcal{N}_{\rm eff}$ as a function of $\Delta m^2$ is a generic feature of all limits. For $E_\nu \sim 10\,\mathrm{MeV}$ and $\Delta m^2 = O(10^{-10}\,\mathrm{eV}^2)$ the oscillation length $L_{\rm osc} = 4\pi E_\nu/\Delta m^2$ attains the value of the earth-sun distance, 1 AU. For $\Delta m^2 > 10^{-9}\,\mathrm{eV}^2$ the oscillation becomes rapid so that $\sin^2[\Delta m^2 L/(4E_\nu)] \to 1/2$ and all limits turn into horizontal lines, independent of $\Delta m^2$.

#### *XENON10, XENON100*

Before LUX, XENON100 [30, 31] set the most stringent limits on DM scattering via spin-independent scattering. However, for the $\nu_b$ model, the low-energy ionization-only analysis by XENON10 [9] with a pre-cut exposure of 15 kg days turned out to be the most constraining experiment. This is due to the steeply falling recoil spectrum a practically massless particle of MeV energies can induce.

Here we improve on our previous analysis in two significant ways. First, for XENON100 the final data set with an exposure of $225\,\mathrm{days}\times 34\,\mathrm{kg}$ is published [10]. Since only two events consistent with background are observed, previous sensitivity to $\nu_b$ from 100 live days is approximately doubled. Second, the XENON10 ionization-only low-threshold study underwent some revision by the collaboration. Importantly, systematic errors of $Q_y$ have been assessed in [32]. We can now derive a limit from XENON10 that is better corroborated. In our previous work, the XENON10 limit was most uncertain of all, due to the delicate sensitivity on $Q_y$ below $E_R < 10\,\mathrm{keV}$ for which $Q_y$ is poorly known.

Our derivation of XENON100 limits is based on a 99.75% ER rejection cut and is in methodology similar to our previous analysis [4]. Therefore, in contrast to LUX, we are not required to model ER background. Two events remain in the final data-set; they are consistent with a background expectation of $(1\pm0.2)$ [10]. The S1 signal is computed using the parameterization of $\mathcal{L}_{\rm eff}$ given in [31] which is based on the measurements of [33]. In accordance with our previous analysis [4], we extrapolate $\mathcal{L}_{\rm eff}$ linearly to zero from 3 keV to 2 keV.[3] We

[3] If we adopt instead the more conservative approach and refrain from modeling nuclear recoils below 3 keV the resulting limit

take into account Poisson fluctuations in S1 and set the analysis threshold to 3 PE in accordance with [10]. New cut acceptances are found in Fig. 1 of the latter paper and $L_y = (2.28 \pm 0.04)$ is a value updated in the same reference; $S_e = 0.58$, $S_n = 0.95$, and $Y = 19.5$ PE. The two observed events had $S1 = 3.3$ PE and 3.8 PE. Using Yellin's maximum gap method [34] we set an upper limit on the $\nu_b$ signal strength. The resulting constraint is shown in Fig. 3.

We now turn to XENON10. The S1 signal is discarded so that with the S2-only analysis a lower threshold of $E_R = \mathcal{O}(1\,\mathrm{keV})$ can be reached—at the expense of additional background. In an early revision by the collaboration, a position cut was discarded so that the number of events in the energy window between ∼1.4-10 keV increases from 7 to 23 with effective exposure more than doubled, from 6.2 kg days to 13.8 kg days; Fig. 2 in [9]. In addition, the new analysis in [32] quantifies potential systematic errors in $Q_y$, and hence in the calibration of nuclear recoil energy, for $E_R \gtrsim 3\,\mathrm{keV}$. Here we derive the limit based on $Q_y$ shown in Fig. 3 of [32]. For this, we group the observed events into three bins of 5–32 ionized electrons, $\{n_e^{\min}, n_e^{\max}, N_{\rm obs}\}$, namely, $\{5, 8, 2\}$, $\{8, 16, 5\}$, and $\{16, 32, 9\}$ with a total number of 16 events observed. The computation of S2 then proceeds similarly to S1 above where we account for Poisson fluctuations in the number of ionized electrons. A final extrapolation of $Q_y(E_R)$ to $E_R(5\,e^-)$ is necessary. We assume a flat trend. Varying $Q_y$ within its $\pm 1\sigma$ error band with the same extrapolation changes the limit only very mildly within $\Delta\mathcal{N}_{\rm eff} < 10$. The exclusion limit based on the binned data set is derived identically as in the LUX case.

### CDMS-Si

A blind analysis by the CDMS-II collaboration of 140.2 kg-days of data collected with their silicon detectors revealed three DM-candidate events with a total expected background of 0.7 [5]. When including the spectral information of the observed events, the background-only hypothesis has a 0.19% probability when compared to one which includes the signal of a WIMP with spin-independent cross section of $1.9 \times 10^{41}\,\mathrm{cm}^2$ and mass 8.6 GeV. This interpretation of CDMS-Si result is intriguing but is now severely challenged by the null-observation of LUX, where more than $10^3$ events were expected at the CDMS best fit point [29]. Here we offer an alternative explanation of the observed excess that at this point stands unchallenged by LUX.

becomes instead weaker with respect to [4]. This demonstrates the great sensitivity on $\mathcal{L}_{\rm eff}$ given the soft recoil spectrum $\nu_b$ induces for xenon.

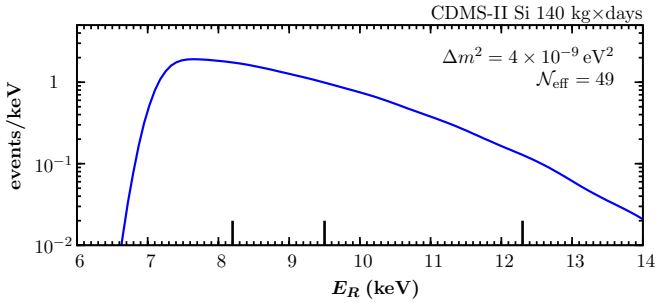



FIG. 1: Fit of the three silicon events in CDMS-II; the recoil locations of the events are indicated by the vertical bars at the bottom of the figure.

We fit the tree events using 1 keV bins starting from 7 keV which corresponds to the lowest threshold of all detectors untill 15 keV above which no signal from $\nu_b$ is induced. The overall efficiency is taken from Fig. 1 of [5]. The best fit is inferred from minimizing the Poisson log-likelihood ratio

$$\chi^2 = 2 \sum_{\text{bins } i} \left[ y_i - n_i + n_i \ln\left(\frac{n_i}{y_i}\right) \right], \qquad (13)$$

where the last term absent for zero observed events, $n_i = 0$, $y_i$ is expected number of events. The minimum in $\chi^2$ is attained for,

$$\mathrm{CDMS-Si}: \Delta m^2 = 4 \times 10^{-9}\,\mathrm{eV}^2,\ \mathcal{N}_{\rm eff} = 49 \qquad (14)$$

with $\chi^2/n_d = 7/6$. The favored region is shown in Fig. 3. As one can see, there is no special preference for small $\Delta m^2$, and the allowed band can be continued to fairly large values to be cut off only by a modification of neutrino oscillations in short- and long-baseline type of experiments.

### CoGeNT

The CoGeNT experiment [11, 12, 35] employs a p-type point-contact germanium crystal (0.44 kg). It has the advantage of a very low energy threshold 0.5 keVee electron recoil equivalent so that despite a moderately heavy target nucleus ($A = 76$), good sensitivity to light DM in the 10 GeV-ballpark or to $\nu_b$ is expected. Indeed, the collaboration reports an unexplained quasi-exponential rise at lowest energies.[4] The origin of it is unknown and has lead to the speculation of a DM signal with favored mass in the $\sim 8 - 10$ GeV. This hypothesis is now seriously challenged, if not completely excluded by LUX.

[4] In addition to the signal-rise below 1 keVee the data also appears to be annually modulated in the 0.5–3.2 keVee bracket which we do not address here.

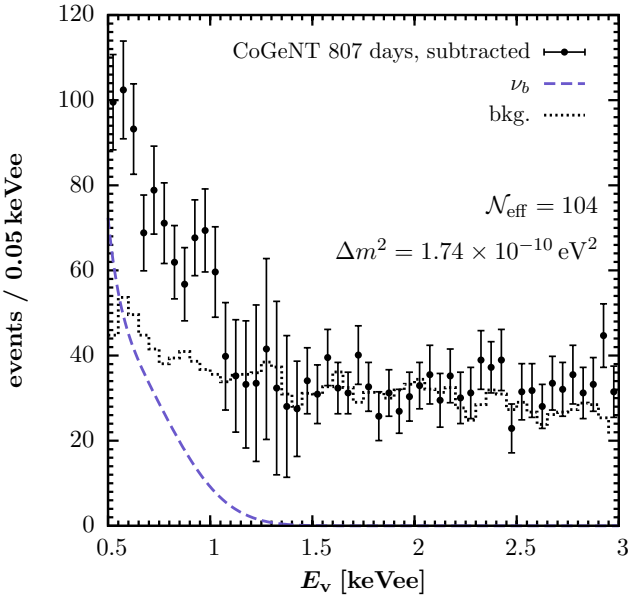



FIG. 2: Fit to the CoGeNT 807 live-day spectrum. The data points show the signal after subtraction of cosmogenic radioactive background. The dotted line represents the best understanding of backgrounds according to [12]; when the dashed line from $\nu_b$ is added is a good fit to the black data points is obtained.

The drawback of the experiment is that it registers ionization from both, nuclear recoils and electromagnetic background without being able to discriminate between the two. Already at the time of our previous analysis [4], it was clear that incomplete charge collection on the surface induces a potential background that mimics a signal in $\nu_b$. Hence in [4] reliable ROIs could not be provided. Instead, an envelope that limits $\mathcal{N}_{\rm eff} \lesssim 200$ was established. It indicated the region of "compatibility" with the other anomalies. Larger values of $\mathcal{N}_{\rm eff}$ lead to signal strengths in excess of the observed data.

In [12] the collaboration provides a detailed discussion of backgrounds. Therefore, we are now able 1) to infer ROIs that are based on a better, quantitative understanding of backgrounds and 2) to use a data set which almost has twice the exposure of that of our previous analysis (807 vs. 442 kg days). The data together with the background model are taken from Fig. 23 of [12] and are respectively reproduced by the points and dotted line in Fig. 2. The spectrum is corrected for efficiencies and cut acceptance; cosmogenically induced radioactive backgrounds have been subtracted. We use Lindhard theory to convert nuclear recoil energies to ionization signal that is calibrated with gamma radiation, $E_{\rm v}({\rm keVee}) = Q \times E_R({\rm keV})^{1.1204}$. The quenching factor is $Q = 0.19935$ and the detector resolution is $\sigma^2 = (69.4\,{\rm eV})^2 + 0.858\,{\rm eV} \times E_{\rm v}({\rm eV})$ [36].

The maximum recoil energy of $^8$B neutrinos on germanium is $E_R \leq 7\,{\rm keV}$ which corresponds to an electron recoil equivalent of $E_{\rm v} \leq 1.76\,{\rm keVee}$. This coincides with the region in which the exponential rise is present and we fit the first 25 data points in that energy interval. With 95% confidence we find two ROIs. The best fit is attained for

$$\text{CoGeNT}: \Delta m^2 = 1.74 \times 10^{-10}\,{\rm eV}^2,\ \mathcal{N}_{\rm eff} = 104 \quad (15)$$

and is shown by the solid (blue) line in Fig. 2. The model provides an excellent description of the data, $\chi^2/n_d = 18/23$. We observe a significant shift of the best-fit ROI with respect to our previous analysis [4]. In the latter, given the absence of quantified backgrounds, the signal-only interpretation favored a best-fit ROI centered around $\mathcal{N}_{\rm eff} = 228$. With the better understanding of backgrounds, the CoGeNT explanation now overlaps with the regions inferred for CDMS-II silicon and CRESST-II.

As one can see, only small fraction of the parameter space of the $\nu_b$ model can explain the CoGeNT excess. In particular, it appears that large values of $\Delta m^2$ are incompatible with current results. This stems from too soft of a recoil for most of the oscillation patterns except the one that gives relative enhancement to the most energetic part of $^8$B spectrum, yielding events with $E_{\rm v} \sim 1\,{\rm keVee}$. It must be said that if the current model of background introduces some spectral distortion, and the excess is actually *softer* than appears in Fig. 2, then the available parameter space can be significantly enlarged, with $\Delta m^2$ in excess of $10^{-9}\,{\rm eV}^2$ also becoming open for speculative interpretations.

## SIMILARITY WITH LIGHT-DM

It is known that light DM and $^8$B neutrinos from the sun can induce recoil spectra in direct detection experiments that are similar in morphology. Hence a positive signal of either origin may be confused with one of the other. The ballpark of DM masses $m_{\rm DM}$ where this is the case can be found by comparing the DM maximum recoil energy $E_R^{\rm max} = 2m_{\rm DM}^2 v^2/m_N$ ($m_{\rm DM} \ll m_N$) with the one from neutrinos, $E_R^{\rm max} = 2E_\nu^2/m_N$. Hence, $m_{\rm DM} \approx E_\nu/v = O(8)\,{\rm GeV}$ for typical values of $E_\nu$ and the DM-target relative velocity $v$. This similarity of signal is illustrated in Fig. 4 for a projected CRESST-II data set on a $CaWO_4$ target.

In the following the two alternative hypotheses for a potential signal in future direct detection experiments are explored. The $\nu_b$ model is very predictive once the oscillation length becomes smaller than the earth-sun distance. The only free parameter is then $\mathcal{N}_{\rm eff}$ and it renormalizes the signal strength. A straightforward approach is to generate recoil spectra from $\nu_b$ (the underlying true hypothesis) and ask the question: How easily are the observed data confused with a detection of light DM (the alternate hypothesis)?

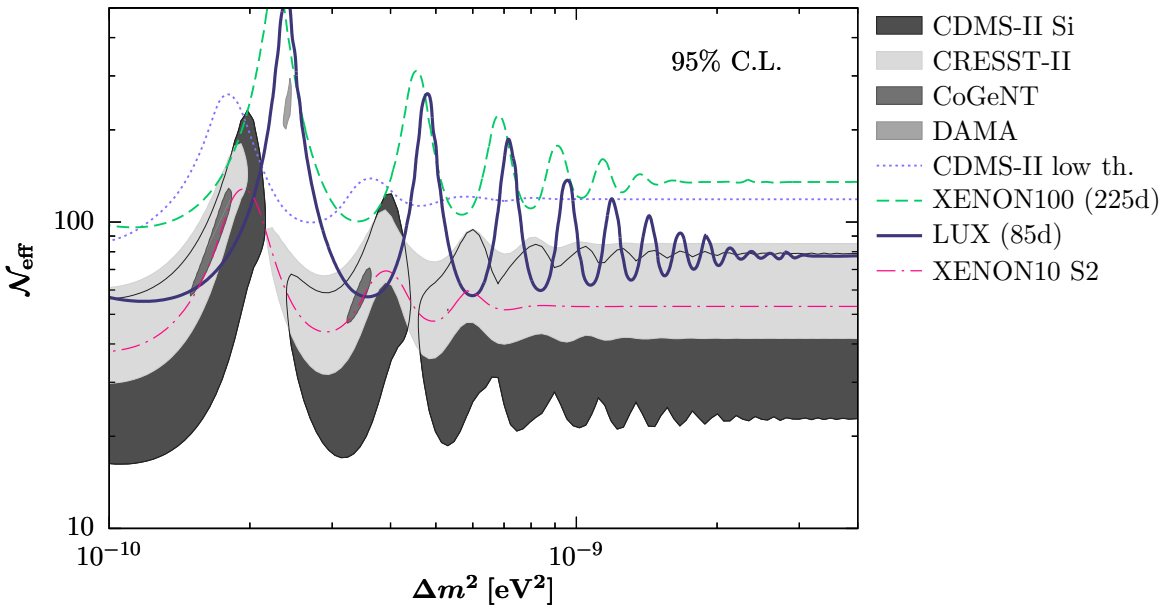



FIG. 3: Summary plot of direct detection favored regions and constraints in the parameters $\Delta m^2$ and $\mathcal{N}_{\rm eff}$ at 95% confidence. *Favored regions:* the broad (dark) light shaded gray band shows the CDMS-Si (CRESST-II) regions. The two small shaded islands are the regions in which the CoGeNT excess is explained. In the medium gray shaded island DAMA's modulation amplitude is fitted; the phase, however, remains significantly discrepant by about one month. *Constraints:* $\mathcal{N}_{\rm eff}$ values above the various lines are excluded with 95% confidence. From top to bottom at $\Delta m^2 > 10^{-9}\,{\rm eV}^2$ the respective constraints are from XENON100, from CDMS-II low-threshold data, from LUX, and from XENON10.

To quantitatively answer this question we produce mock sets of data for various target nuclei for the exemplary values $\Delta m^2 = 10^{-9}\,{\rm eV}^2$ and $\mathcal{N}_{\rm eff} = 30$. In anticipation of a future superCDMS setup where some fraction of detectors are made from silicon, we generate spectra for Ge and Si with nuclear recoil energies in the interval $E_R = 5 - 8\,{\rm keV}$ and bin-size of 0.5 keV and respective exposures of 20 kg-yr and 100 kg-yr. With the chosen parameters, the total number of events in Ge (Si) is 45 (1268). For germanium 90% of events are located in the first bin so that in contrast to silicon, rather limited spectral information is available.

In addition to superCDMS, we also provide projections for the CRESST-II upgrade that is—at the time of writing—taking data. New detector designs have been developed and show promising results in the elimination of previously encountered Pb and $\alpha$ backgrounds [37]. The projected joint exposure of their $CaWO_4$ detectors of a 2 year run is 2000 kg-days with the potential to conclusively test its own anomaly. We generate a mock spectrum from $\nu_b$ with same neutrino parameters as above but with a higher threshold of 10 keV, which more closely resembles the experimental reality. The spectrum in oxygen extends to higher recoil energies with a total number of 36 expected events in 10 bins in the energy interval $10 - 20\,{\rm keV}$, all of which are oxygen recoils.

The binned spectra are then fitted to a canonical light DM model with spin-independent WIMP-nucleon cross section $\sigma_n$ using (13). We choose a Maxwellian DM velocity distribution with escape speed $v_{\rm esc}$ and most probable velocity $v_0 = 220\,{\rm km/s}$. The goodness-of-fit serves as the test statistic for the DM hypothesis, *i.e.* DM is considered as the null hypothesis and we (falsely) accept it for a p-value $p > 5\%$. The result of the fit is shown by the shaded regions in Fig. 5 for $v_{\rm esc} = 544\,{\rm km/s}$ [38]. Outside of them, the probability to confuse the $\nu_b$ signal with light DM from the observation in either Ge, Si, or O is less than 5%. Also shown are current limits on the SI cross section from LUX and CDMSlite [39]. In order to quantify the dependence on the velocity distribution in the regions enclosed by the thin gray lines $v_{\rm esc}$ is allowed to float in the range $450 \leq v_{\rm esc}({\rm km/s}) \leq 650$; of course, the same halo parameters will hold for Ge and Si so that no effective broadening as indicated by the thin gray lines takes place in reality. Rather, the thin lines indicate the "comfort zone" in which the ROI can move around for the Maxwellian halo model.[5]

The first observation is that all shaded regions are disjoint. As alluded before, the spectrum in Ge falls steeply

[5] The reason why the lines intersect slightly with their associated shaded regions is because in the former (latter) case the goodness-of-fit statistic follows a $\chi^2$ distribution with $N_{\rm bins} - 3$ ($N_{\rm bins} - 2$) degrees of freedom; the limits from LUX and CDMSlite are nominal ones—they too will be affected by changes in $v_{\rm esc}$.

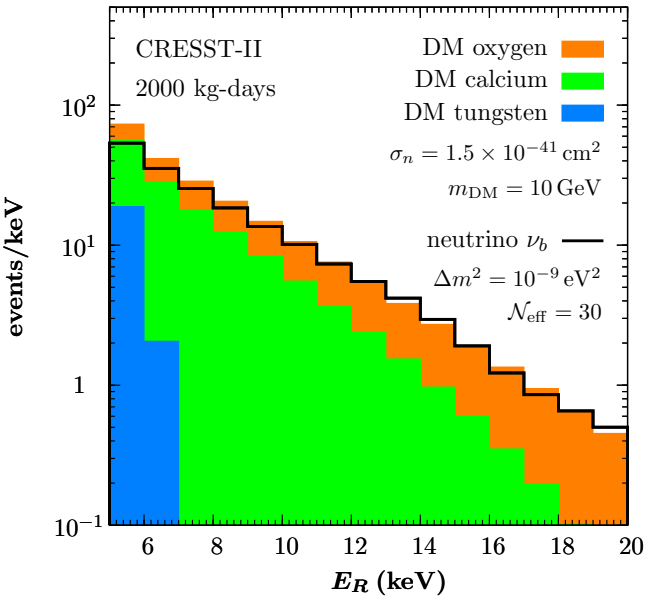



FIG. 4: Comparison of theoretical recoil spectra from $\nu_b$ with $\mathcal{N}_{\mathrm{eff}} = 30$, $\Delta m^2 = 10^{-9}\,\mathrm{eV}^2$ and from DM with $m_{\mathrm{DM}} = 10\,\mathrm{GeV}$, $\sigma_n = 1.5 \times 10^{-41}\,\mathrm{cm}^2$, and $v_{\mathrm{esc}} = 544\,\mathrm{km/s}$ in a future CRESST-II data set. Above $E_R = 10\,\mathrm{keV}$ (a realistic threshold of the experiment) all $\nu_b$ recoils are on O.

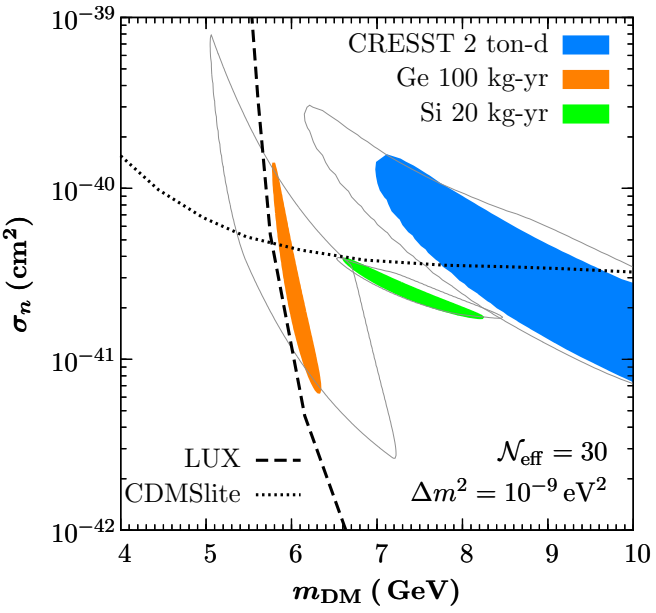



FIG. 5: Dark matter interpretation of a positive $\nu_b$ signal with $\mathcal{N}_{\mathrm{eff}} = 30$ and $\Delta m^2 = 10^{-9}\,\mathrm{eV}^2$ in a future (idealized) superCDMS-type direct detection experiment equipped with Ge and Si targets as well as for the new run by the CRESST-II dark matter search. The exposures are 20 (100) kg-yr for Si (Ge) and 2000 kg-days for $CaWO_4$. Inside the shaded regions, the DM hypothesis is (falsely) accepted with p-value $p > 5\%$ by the goodness-of-fit criterion. From the disjointness of the regions DM and $\nu_b$ can be discriminated which stresses the importance of employing multiple targets. Inside the parameter regions, enclosed by the thin gray lines, the DM escape velocity is allowed to vary between $450 \leq v_{\mathrm{esc}}(\mathrm{km/s}) \leq 650$, indicating the areas of parameter space in which the shaded regions can move for the Maxwellian halo model. The LUX and CDMSlite exclusion limits are as reported by the collaborations.

and has little statistics. Therefore a light DM particle of mass $m_{\mathrm{DM}} \simeq 6\,\mathrm{GeV}$ is selected. Exponential sensitivity in the mass translates into a region in WIMP-nucleon cross section that can vary by one order in magnitude, $\sigma_n \sim 10^{-41} - 10^{-40}\,\mathrm{cm}^2$. With much more statistics the ROI in Si is significantly smaller and favors heavier DM. A more shallow signal yields a bigger allowance in $m_{\mathrm{DM}} \simeq 7 - 8\,\mathrm{GeV}$ but selects a more narrow range of cross sections, $\sigma_n \sim 2 - 3 \times 10^{-41}\,\mathrm{cm}^2$, and which serves to normalize the rate. Finally, recoils on O in a future CRESST-II data set contain both features: small statistics gives a relatively accommodating region in parameter space and a shallow spectrum that allows for a very broad range in DM mass. The fact that the ROI are largely disjoint stresses the importance of employing multiple targets in direct detection. It breaks the degeneracy between these two alternative new physics interpretations.

Forecasts can also be made for the liquid scintillator experiments such as XENON1T or future exposures of LUX. For the xenon target, the maximum recoil energy of $^8$B neutrinos is $E_R \leq 4.5\,\mathrm{keV}$ so that the most promising avenue lies in the exploration of ionization-only, low-threshold studies. To a fair extent, we have covered this ground in our previous paper [4] where we showed the projections for XENON100 and that can be rescaled for larger exposures. The finding was that better sensitivity is mostly limited by ER backgrounds. For the XENON100 detector they are at the level of $10^{-2}\,\mathrm{cpd/kg/keV}$ [40]; the LUX measured ER rate in the fiducial volume in the keV-regime is now $3 \times 10^{-3}\,\mathrm{cpd/kg/keV}$ [6]. Therefore, we do not expect immediate drastic improvements so that we refrain from repeating a similar analysis here but instead await new data from the experiments.

The analysis presented here can be further extended and improved: First, in CRESST-II, the phonon measurement provides a nuclear recoil energy scale so that the quenching of the scintillation light signal allows for a (limited) discrimination between recoils on Ca, O, or W. The $\nu_b$ model does not induce W-recoils (and no Ca recoils for $E_R > 10\,\mathrm{keV}$, as can be seen from Fig. 4) so that further differential information is available that will help to scrutinize the model from light WIMPs. The discrimination of nuclear bands works better of high recoil energies and it becomes a quantitative question how well this can be done in practice. Second, the generation of the $\nu_b$ signal was done under idealized circumstances. Poisson fluctuations in the generation of the mock spectrum

have not been taken into account. This can be achieved in Monte-Carlo-type analyses in which a large sample of initial spectra is generated. Our conclusions will not be affected by this. The ROI in Fig. 5 may broaden somewhat but the goodness-of-fit test already "knows" about the statistical error bar so that all qualitative features will remain. More detailed explorations of this sort and the comparison with other halo models are left for future work.

## CONCLUSIONS

In this work we have re-visited the model of a new neutrino state that has no charged current interaction with matter, but has a new neutral-current-type force with baryonic charge. If the strength of the interaction is chosen to be two orders of magnitude above the strength of the SM weak force, an important experimental probe of this model is the coherent scattering of neutrinos on nuclei. When the mass splitting is small, *e.g.* $\Delta m^2 \ll \Delta m^2_\odot$, no significant flux of new neutrinos must be produced in the terrestrial neutrino beam experiments, and consequently the enhanced interaction of new neutrinos is not as constrained as it may naively seem. However, the mixing of $n_4$ with the SM massive state $n_2$ can easily lead to a finite oscillation probability for the solar neutrino flux, with observable consequences for the rare underground event searches, and especially for the Dark Matter direct detection experiments.

A region of the WIMP parameter space with mass range of a few GeV and cross section of few$\times 10^{-41}$ cm$^2$ per nucleon has attracted enormous amount of attention in recent years, due to a number of experimental results that can be interpreted as positive evidence for the recoil signal. However, following the release of the first LUX results [6], the explanation of direct detection anomalies via light DM models are now thoroughly disfavored. In contrast, we find that the elastic scattering of $\nu_b$ is still an attractive candidate for explaining most of the anomalies, capable of a simultaneous fit to the CDMS-II silicon [5], CoGeNT [12], and CRESST-II [13] excess of events. The conclusion about the viability of the model is based on our computation of the LUX limit on $\nu_b$, and the update of limits from XENON100 using the final data set [10], as well as from XENON10 with a better understanding of systematic uncertainties in the charge yield from nuclear recoils [32].

Since the model of $\nu_b$ is very predictive in the most relevant region of parameter space, we expect that in the coming years it will be decisively tested. Irrespective of current anomalies, our investigation offers a future path for distinguishing between light-DM and neutrino recoil signals. Indeed, the ongoing low-background run of CRESST-II [37], as well as the planned expansion of the CDMS program (superCDMS [14]) will have the potential to do so, and in a way that is free from the uncertainties in the low-energy recoil response, liquid xenon experiments are prone to.

Finally, while the $\nu_b$ model, as shown in this paper, is getting constrained at an interesting level by DM direct detection experiments, there are complementary ways of exploring the same model. In proton-on-target type of experiments such as MiniBooNE [41], the pair-production of $\nu_b\bar{\nu}_b$ can be studied. The $\nu_b$ appearance in the solar neutrino flux can also be directly constrained at a very interesting level by the search of carbon excitation lines in Borexino data [42].

JP would like to thank L. Dai, M. Kamionkowski, and I. Shoemaker for discussions on various aspects of the baryonic neutrino model.


[1] M. W. Goodman and E. Witten, Phys. Rev. D **31**, 3059 (1985).
[2] M. Pospelov, Phys.Rev. **D84**, 085008 (2011), 1103.3261.
[3] R. Harnik, J. Kopp, and P. A. Machado, JCAP **1207**, 026 (2012), 1202.6073.
[4] M. Pospelov and J. Pradler, Phys.Rev. **D85**, 113016 (2012), 1203.0545.
[5] R. Agnese et al. (CDMS Collaboration), Phys.Rev.Lett. (2013), 1304.4279.
[6] D. Akerib et al. (LUX Collaboration) (2013), 1310.8214.
[7] M. I. Gresham and K. M. Zurek (2013), 1311.2082.
[8] E. Del Nobile, G. B. Gelmini, P. Gondolo, and J.-H. Huh (2013), 1311.4247.
[9] J. Angle et al. (XENON10), Phys.Rev.Lett. **107**, 051301 (2011), 1104.3088.
[10] E. Aprile et al. (XENON100 Collaboration), Phys.Rev.Lett. **109**, 181301 (2012), 1207.5988.
[11] C. Aalseth, P. Barbeau, J. Colaresi, J. Collar, J. Diaz Leon, et al., Phys.Rev.Lett. **107**, 141301 (2011), 1106.0650.
[12] C. Aalseth et al. (CoGeNT Collaboration), Phys.Rev. **D88**, 012002 (2013), 1208.5737.
[13] G. Angloher, M. Bauer, I. Bavykina, A. Bento, C. Bucci, et al., Eur.Phys.J. **C72**, 1971 (2012), 1109.0702.
[14] D. Akerib, M. Attisha, C. Bailey, L. Baudis, D. A. Bauer, et al., Nucl.Instrum.Meth. **A559**, 411 (2006).
[15] A. Aguilar-Arevalo et al. (LSND Collaboration), Phys.Rev. **D64**, 112007 (2001), hep-ex/0104049.
[16] A. Aguilar-Arevalo et al. (MiniBooNE Collaboration), Phys.Rev.Lett. **105**, 181801 (2010), 1007.1150.
[17] J. Kopp, P. A. N. Machado, M. Maltoni, and T. Schwetz, JHEP **1305**, 050 (2013), 1303.3011.
[18] C. Giunti and C. W. Kim (2007).
[19] J. Beringer et al. (Particle Data Group), Phys.Rev. **D86**, 010001 (2012).
[20] J. Pradler, Talk given at the INFO 2013 workshop, Santa Fe, NM (2013), URL `http://public.lanl.gov/friedland/info13/INFO13talks.html`.
[21] A. Friedland, M. L. Graesser, I. M. Shoemaker, and L. Vecchi, Phys.Lett. **B714**, 267 (2012), 1111.5331.
[22] B. Dasgupta and J. Kopp (2013), 1310.6337.
[23] A. Drukier and L. Stodolsky, Phys. Rev. D **30**, 2295

(1984).
[24] R. H. Helm, Phys.Rev. **104**, 1466 (1956).
[25] J. N. Bahcall, A. M. Serenelli, and S. Basu, Astrophys.J. **621**, L85 (2005), astro-ph/0412440.
[26] J. N. Bahcall, E. Lisi, D. E. Alburger, L. De Braeckeleer, S. J. Freedman, and J. Napolitano, Phys. Rev. C **54**, 411 (1996), URL http://link.aps.org/doi/10.1103/PhysRevC.54.411.
[27] J. N. Bahcall, Phys. Rev. C **56**, 3391 (1997), URL http://link.aps.org/doi/10.1103/PhysRevC.56.3391.
[28] M. Szydagis, A. Fyhrie, D. Thorngren, and M. Tripathi, JINST **8**, C10003 (2013), 1307.6601.
[29] R. Gaitskell and D. McKinsey, Talk given at the Sanford Underground Research Facility, Lead, SD (2013), URL http://luxdarkmatter.org/talks/20131030_LUX_First_Results.pdf.
[30] E. Aprile et al., Astropart. Phys. **34**, 679 (2011), 1001.2834, URL http://arxiv.org/abs/1001.2834.
[31] E. Aprile et al. (2011), 1104.2549, URL http://arxiv.org/abs/1104.2549.
[32] E. Aprile et al. (XENON100 Collaboration), Phys.Rev. **D88**, 012006 (2013), 1304.1427.
[33] G. Plante, E. Aprile, R. Budnik, B. Choi, K. Giboni, et al., Phys.Rev. **C84**, 045805 (2011), 1104.2587.
[34] S. Yellin, Phys.Rev. **D66**, 032005 (2002), physics/0203002.
[35] C. Aalseth et al. (CoGeNT), Phys.Rev.Lett. **106**, 131301 (2011), 1002.4703.
[36] C. Aalseth et al. (CoGeNT), Phys.Rev.Lett. **101**, 251301 (2008), 0807.0879.
[37] F. Proebst, Talk given at the "Workshop on future Dark Matter Experiments", Vienna, Austria (2013), URL http://indico.cern.ch/conferenceTimeTable.py?confId=259833#
[38] M. C. Smith, G. Ruchti, A. Helmi, R. Wyse, J. Fulbright, et al., Mon.Not.Roy.Astron.Soc. **379**, 755 (2007), astro-ph/0611671.
[39] R. Agnese et al., ArXiv e-prints (2013), 1309.3259.
[40] E. Aprile et al. (XENON100 Collaboration), Phys.Rev. **D83**, 082001 (2011), 1101.3866.
[41] R. Dharmapalan et al. (MiniBooNE Collaboration) (2012), 1211.2258.
[42] G. Bellini et al. (Borexino Collaboration), Phys.Rev. **D82**, 033006 (2010), 0808.2868.